Fast Trap Jaws and Giant Neurons in the Ant *Odontomachus*

Wulfila Gronenberg,* Jürgen Tautz, Bert Hölldobler

Ants of the ponerine genus *Odontomachus* use a trap jaw mechanism when hunting fast prey. When particular trigger hairs, located on the inner edge of the mandibles, are touched by prey, the jaws close extremely rapidly and trap the target. This trap jaw response lasts only 0.33 to 1 millisecond. Electrophysiological recordings demonstrated that the trigger hairs function as mechanoreceptors. Associated with each trigger hair are large sensory cells, the sensory axons of which measure 15 to 20 micrometers in diameter. These are among the largest sensory neurons, and their size implies that these axons conduct information very rapidly.

Speed, an important physical ability of many animal species, is often affected by an evolutionary "arms race" between predators and prey (*1*). During evolution the efficiency with which the predator captures prey should increase, but natural selection should also improve the ability of the prey to escape. This leads to remarkable adaptations and astoundingly fast movements of both predators and prey. Among the extremes are the rapid takeoffs of locusts and flies (within fractions of a second) (*2*), the jumps of fleas (0.7 to 1.2 ms) (*3*) and springtails (4 ms) (*4*), and the escape response of cockroaches (40 ms) (*5*) and fish (35 ms) (*6*). Nevertheless, there are predators that prey on these fast animals. They usually use a stalking or ambushing technique, and they are equipped with fast weapons (*5*, *7*, *8*).

The trap jaw ants have powerful mandibles that are equipped with piercing apical teeth that are used to trap the prey. Such trap jaw techniques have evolved independently in several ant genera (*9*). During an investigation of the trap jaw mechanism in the ponerine genus *Odontomachus*, we discovered that the mandible strike of this ant is among the fastest movements and is controlled by an extremely fast reflex; it is triggered by the stimulation of very thick sensory neurons.

In the Neotropical species *O. bauri*, the mandibles are approximately 1.8 mm long and their interior consists mainly of a large tracheal sac filled with air. This renders the whole structure lightweight, a critical feature for fast acceleration of the jaw. When the ants are hunting, the mandibles are fully opened (Fig. 1). As a result of specializations of the mandible joint, the gaping mandibles are held in a metastable position without further muscular tension (*10*). Powered by huge closer muscles, the cocked mandibles are ready to strike. We analyzed this mandible strike on ants that were fixed at the thorax. The fastest full mandible strike, recorded with high-speed cinematography (3000 frames per second), happened within one film frame (0.33 ms); in those cases the jaws had been closed and were already rebounding after two frames (0.66 ms; see Fig. 2) (*11*). The rapidity of this strike surpasses even the discharge of the cnidarian nematocyst [the hydrozoan "sting cells," the initial "explosion" of which is accomplished within 0.5 ms (*12*)] or the escape jump of the click beetle which takes about 0.6 ms (*13*).

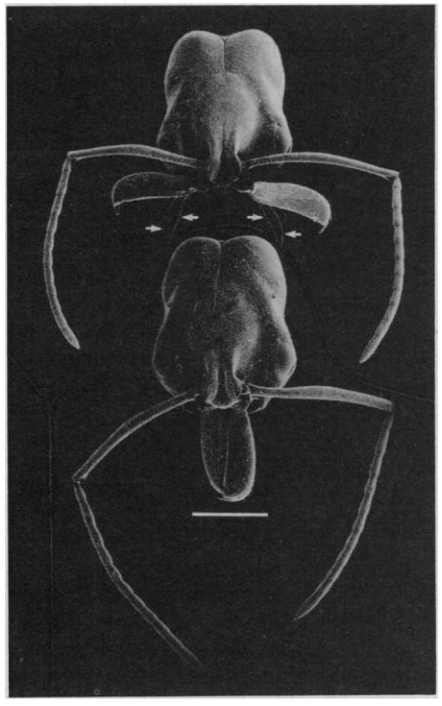

Fig. 1. Scanning electron micrographs of the head of *Odontomachus* sp. with cocked (top) and closed (bottom) mandibles; frontal view. Arrows point at trigger hairs. Bar = 1 mm.

Comparable data were obtained by photoelectric scanning, during which we recorded movements lasting 0.5 ms to more than 1 ms (Fig. 3, A through C). Unlike other fast movements (for example, the jump of locusts or fleas), the mandible strike of *Odontomachus* seems not to be continuously accelerated. Our photoelectric measurements indicate that the strike is slowed down during the last third of its trajectory. This deceleration may protect the mandibles if the strike fails and the mandibles collide with each other.

Before a hunting *Odontomachus* worker releases the trap jaw strike, it locates the prey object with its antennae (*14*), the chemo- and mechanosensory hairs of which convey information on the nature of the encountered object. Once the prey has been identified, the ant jerks forward, so that the prey is touched by long (more than 1 mm) trigger hairs, two of which are located on each mandible. The actual releasing mechanism for the mandible strike is the contact of the hairs with the prey object. We therefore investigated the function and associated structure of these sensilla in detail.

By recording electrical activity arising from these hairs, we were able to demonstrate that they are mechanosensory sensilla. The fast and reliable response consists of a volley of action potentials delivered when the sensilla are touched by an object (*15*). The large sensory cells associated with each trigger hair give rise to large nerve fibers (axons) that run through the mandibular nerve into the subesophageal ganglion (SEG), the part of the central nervous system (CNS) that serves the sensory and motor functions of the mouthparts. We were able to stain the sensory cells with different tracers (*16*) and graphically reconstruct the axons and their collaterals within the CNS, using a camera lucida attachment to the microscope. Within the SEG, each sensory axon forms a huge axon terminal (Fig. 3D). On either side, the axon terminal originating from the lateral trigger hair is restricted to that side while the axon of

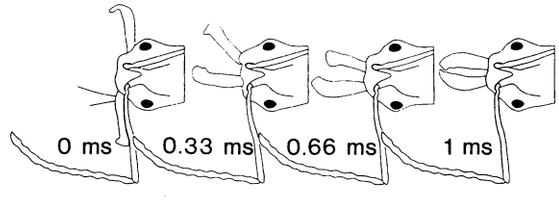

Fig. 2. Outlines of the images redrawn from the original high-speed cinematographs of the mandible movement. Time between frames: 0.33 ms. The strange shape of the mandibles in the second and third drawings reflects the image blur due to the fast motion.

Theodor Boveri Institut, Lehrstuhl für Verhaltensphysiologie und Soziobiologie der Universität, Am Hubland, D-97074 Würzburg, Germany.

*To whom correspondence should be addressed.

the median trigger hair also extends to the opposite side of the SEG. The diameter of the sensory axons (15 to 20 μm) implies that they conduct information at a very high velocity. The bilateral distribution of the axon terminals indicates that the information is simultaneously distributed to both sides of the CNS, which may synchronize the strike of the two mandibles.

Tracing the sensory neurons, we found that the stained axon terminals on either side run in parallel and are in close contact with two very large (unstained) fibers. We have anatomical evidence indicating that these unstained fibers are the axons of motor neurons that supply the mandible muscles (*17*). Judging from light microscopy, we believe that the close proximity between the sensory and the motor neurons would indicate a monosynaptic connection between them, generally the neuronal basis for the fastest possible reflex arc.

As has been shown for other fast movements (*18*), a co-contraction of antagonistic muscles may be involved in the mandible strike of *Odontomachus*, because no muscle is known to respond fast enough to control such an event. Recordings of the electrical activity of the powerful closer muscles show that they are active before but not during the actual mandible strike (Fig. 3, E through G), thus powering or cocking the mandibles before the strike is released. The actual release of the strike is accompanied by smaller and faster muscle potentials (arrows in Fig. 3G), the origin of which we do not yet know.

We speculate that there may be either specialized fast motor units within the large closer muscle or a separate "trigger" muscle that unlocks the joint, thus starting the mandible strike and releasing the energy stored within the head capsule. This may involve resilin, a highly elastic insect protein optimally adapted for the storage of mechanical energy (*19*). If resilin is involved in the mandible strike of *Odontomachus*, it would most likely be localized in the tendon between the mandible closer muscle and the mandible. Some fast insect systems do not rely on resilin but store mechanical energy by virtue of the springiness of sclerotized cuticle alone (*2*).

The trap jaw mechanism of *Odontomachus* resembles that of a cocked spring. The energy for the strike is stored and accumulated over a considerable time and then suddenly is released in a catapult-like action upon contact with the trigger hairs.

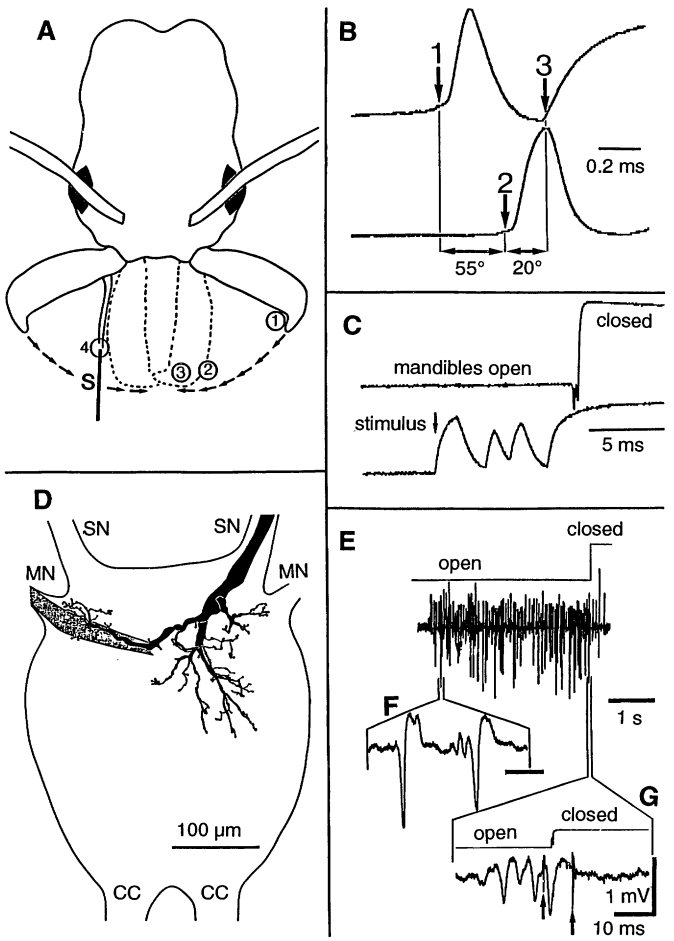

Fig. 3. The mandible movement. (**A**) Experimental setup: phototransistors 1 through 3 scan different points along the track of the moving mandible; phototransistor 4 records the time when the stimulator S touches a trigger hair. (**B**) Mandible strike as revealed by the output of the phototransistors depicted in (A). Arrow 1: shortly after the onset of motion; arrow 2: 55°; arrow 3: an additional 20° further toward the midline. Time elapsed between arrows 1 and 2: 0.3 ms; between arrows 2 and 3: 0.2 ms (resulting in angular velocities of 180°/ms and 100°/ms, respectively). (**C**) Latency between stimulus onset (arrow in lower trace) and mandible movement (upper trace). Vibrations occurring after the stimulator touched the trigger hair cause the repeated peaks in the lower trace. Latency from stimulus onset to completed mandible closure: 8 ms. (**D**) Graphical reconstruction (dorsal view) of the afferent axon (solid profiles) arising from the mechanosensory cell associated with the median trigger hair of the right mandible. This neuron enters the subesophageal ganglion (thin lines) through the sensory mandibular nerve SN. It was traced using biocytin and revealed by avidin–horseradish peroxidase. Stippled profile indicates a motor neuron presumably supplying the left mandible closer muscle by way of the mandibular motor nerve MN. The cervical connectives CC descend to the thoracic ventral nerve cord. (**E** through **G**) Motor activity recorded from the mandible closer muscle before and during a mandible strike. (E) Large, slow action potentials occur preparatory to the strike [depicted at expanded temporal resolution in (F)] and probably provide tension for the snap mechanism while fast spikes are associated with the actual mandible closure [marked by arrows in inset (G), expanded time scale]. Upper traces in (E) and (G): record of mandible movement as described in (B) and (C); bar in (F) = 10 ms.

REFERENCES AND NOTES

1. R. Dawkins and J. R. Krebs, *Proc. R. Soc. London Ser. B* **205**, 489 (1979); J. R. Krebs and N. B. Davies, *An Introduction to Behavioral Ecology* (Sinauer, Sunderland, MA, 1981).
2. H. C. Bennet-Clark, in *The Insect Integument*, H. R. Hepburn, Ed. (Elsevier, Amsterdam, 1976), pp. 421–443.
3. H. C. Bennet-Clark and E. C. A. Lucey, *J. Exp. Biol.* **47**, 59 (1967).
4. E. Christian, *Zool. Jahrb. Abt. Allg. Zool. Physiol. Tiere* **83**, 457 (1979).
5. J. C. Camhi, *Neuroethology* (Sinauer, Sunderland, MA, 1984), p. 79.
6. R. C. Eaton, W. A. Lavender, C. M. Wieland, *J. Comp. Physiol.* **144**, 521 (1981).
7. The praying mantis snatches a fly within 42 ms [H. Maldonado, L. Levin, J. C. Barros Pita, *Z. Vergl. Physiol.* **56**, 237 (1967)], and mantid shrimps strike their legs within 10 ms into their prey [M. Burrows, *ibid.* **62**, 362 (1969)].
8. Some staphylinid beetles "shoot" their tongues at springtails within 1 to 3 ms [T. Bauer and M. Pfeiffer, *Anim. Behav.* **41**, 819 (1991)].
9. M. W. Moffett, *Natl. Geogr. Mag.* **175**, 394 (1989); *Insectes Soc.* **33**, 85 (1986); for review, see B. Hölldobler and E. O. Wilson, *The Ants* (Belknap Press, Cambridge, MA, 1990).
10. R. Barth, *An. Acad. Brasil. Ciencias* **32**, 379 (1960).
11. Not only are the times needed for the mandible strike very short; the angular velocity of the mandible is equally impressive: 180°/ms in Fig. 3B or 270°/ms when the strike is completed within one frame of the high-speed film (Fig. 2). With such an angular velocity, the speed of the mandible tip of *O. bauri* (which is 1.8 mm long) amounts to 8.5 m/s.
12. T. Holstein and P. Tardent, *Science* **223**, 830 (1984).
13. M. E. G. Evans, *J. Zool. (London)* **169**, 181 (1973).
14. N. F. Carlin and D. S. Gladstein, *Psyche* **96**, 1 (1989).
15. W. Gronenberg and J. Tautz, *J. Comp. Physiol.*, in press.
16. The dyes used for tracing the sensory neurons were cobalt chloride, the fluorescent dye Lucifer yellow, or biocytin. The neurons were revealed with avidin coupled to horseradish peroxidase or to fluorescent markers such as Cascade blue. For details see W. Gronenberg and C. Peeters, *Cell Tissue Res.*, in press.
17. On either side, these putative motor axons leave the CNS through a nerve known in other ants as the mandible motor nerve. We were able to trace the two axons to the big mandible closer muscles.
18. Among the fast movements for which cocontrac-

tion of antagonistic muscles has been demonstrated are the locust escape jump [R. H. J. Brown, *Nature* **214**, 939 (1967)] and the predatory strike of the dragonfly larva [Y. Tanaka and M. Hisada, *J. Exp. Biol.* **88**, 1 (1980)] or of the mantid shrimp [M. Burrows, see (*7*)].

19. We thank S. O. Andersen for his advice suggesting that the tendon between the mandible and its closer muscle would be the most probable region in which to find energy-storing materials such as resilin. We also thank the German Institute for the Scientific Film (IWF), where the high-speed cinematography was carried out. Supported by funds from the Deutsche Forschungsgemeinschaft (Leibniz Preis to B.H., SFB 251/project 18, and Gr 933/3).

15 June 1993; accepted 12 August 1993

FMR1 Protein: Conserved RNP Family Domains and Selective RNA Binding

Claude T. Ashley Jr., Keith D. Wilkinson, Daniel Reines, Stephen T. Warren*

Fragile X syndrome is the result of transcriptional suppression of the gene *FMR1* as a result of a trinucleotide repeat expansion mutation. The normal function of the *FMR1* protein (FMRP) and the mechanism by which its absence leads to mental retardation are unknown. Ribonucleoprotein particle (RNP) domains were identified within FMRP, and RNA was shown to bind in stoichiometric ratios, which suggests that there are two RNA binding sites per FMRP molecule. FMRP was able to bind to its own message with high affinity (dissociation constant = 5.7 nM) and interacted with approximately 4 percent of human fetal brain messages. The absence of the normal interaction of FMRP with a subset of RNA molecules might result in the pleiotropic phenotype associated with fragile X syndrome.

Fragile X syndrome is an X-linked dominant disorder with reduced penetrance that occurs at a frequency of approximately 0.5 to 1.0 per 1000 males and 0.2 to 0.6 per 1000 females (*1*). Fully penetrant males exhibit moderate mental retardation along with a phenotype consisting of macroorchidism (enlarged testes), subtle facial dysmorphia, and mild connective tissue abnormalities (*2*). Female patients typically are less severely affected, showing little or no somatic signs and only borderline to mild mental retardation. The molecular basis of fragile X syndrome has been attributed to the expansion of an unstable CGG trinucleotide repeat in the 5′ untranslated region of the gene *FMR1* (*3, 4*).

In fragile X syndrome, when the size of the CGG repeat is in the affected range beyond 230 repeats, the *FMR1* gene is methylated; this methylation results in transcriptional silencing (*5*). The absence of *FMR1* message and its encoded protein, FMRP, is believed responsible for the phenotype of the fragile X syndrome. In addition to the common mutational change of repeat expansion, three variant patients with the clinical presentation of fragile X syndrome have been reported: two males with large deletions encompassing the *FMR1* locus and a severely affected male with a *FMR1* Ile^{304}→Asn missense mutation (*6*).

Alternative splicing generates several isoforms of FMRP with a major species of 69 kD (*7*). Although predominantly cytoplasmic, occasional nuclear localization is observed (*8*). In situ hybridization with *FMR1* mRNA reveals widespread but not ubiquitous expression with abundant message present in the testes and in neurons in the brain (*9*).

Initial analyses of *FMR1* and the predicted protein sequence revealed little sequence similarity to known proteins or motifs. Further analyses of the human and mouse genes, particularly with the use of searches of limited regions of 200 to 400 amino acids in length, revealed two similar regions of FMRP that also were similar to 6 repetitive domains in the yeast protein HX and 14 domains of the chicken gene vigillin (*VIG*) (*10*). Alignments of these amino acid sequences and a resulting profile search revealed a number of proteins containing 1 to 14 repeats of an uninterrupted, 30–amino acid domain (Fig. 1A). Proteins containing this domain, termed KH domains, are believed to constitute a ribonucleoprotein (RNP) family (*11*) that includes mer1, a yeast protein involved in meiosis-specific alternative splicing (*12*); bacterial polynucleotide phosphorylase, which binds RNA and has phosphorolysis activity (*13*); and the highly conserved ribosomal protein S3 (RP S3) (*14*). Thus, most functional aspects of RNA-protein interactions are represented among KH domain–containing proteins, including RNA catalysis, message processing, and translation.

The two KH domains of FMRP reside in the middle of the protein (Fig. 1B), a

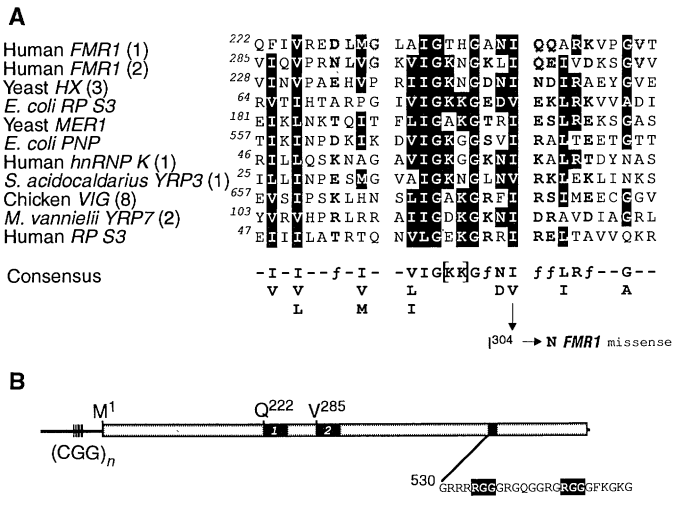

Fig. 1. Location and homologies of RNP family domains in FMRP. (**A**) Alignment (*27*) of the amino acid sequences that make up the KH domains of FMRP and several other proteins and the corresponding consensus sequence. Numbers in parentheses indicate the particular domain shown for the proteins that have multiple KH domains, and the number preceding the first residue indicates that position in the corresponding protein. Dark highlighting indicates similarities among all proteins, whereas stippled highlighting indicates similarity between the two KH domains of FMRP. Boldface residues show the positions of polar amino acids, indicated by *f* in the consensus sequence. The bracketed lysine (K) residues indicate this amino acid at either position in the domain. The position of the isoleucine-to-asparagine mutation at position 304 (I^{304}→N) in a patient (*6*) is indicated at the bottom. (**B**) Diagram of FMRP [residue numbers are as described (*7*)]. The CGG repeat and initiating codon (M^1) are indicated as is each KH domain, labeled 1 and 2. Also shown is the amino acid sequence with the two RGG box domains highlighted. Abbreviations for the amino acid residues are: A, Ala; C, Cys; D, Asp; E, Glu; F, Phe; G, Gly; H, His; I, Ile; K, Lys; L, Leu; M, Met; N, Asn; P, Pro; Q, Gln; R, Arg; S, Ser; T, Thr; V, Val; W, Trp; and Y, Tyr.

C. T. Ashley Jr., K. D. Wilkinson, D. Reines, Department of Biochemistry, Emory University School of Medicine, Atlanta, GA 30322.
S. T. Warren, Howard Hughes Medical Institute and Departments of Biochemistry and Pediatrics, Emory University School of Medicine, Atlanta, GA 30322.
*To whom correspondence should be addressed.